AMO - Advanced Modeling and Optimization, Volume 9, Number 2, 2007

COMPUTATIONAL FLUID DYNAMICS APPLIED TO THERMOCAPILLARY CONVECTION DURING FLOATING CRYSTAL GROWTH OF SILICON

R. YOUNSI[1], A. HARKATI[2], & D.OUADJAOUT[3]

[1] Applied Sciences Department, University of Quebec at Chicoutimi, G7H2B1 Chicoutimi (QC), Canada
[2] Theoretical Physics Laboratory, Physics institute, USTHB, Algiers (Algeria)
[3] Simulation's Laboratory, UDTS, 2Bd Frantz Fanon, Algiers (Algeria)

Abstract

In this article we present numerical results concerning the simulation of semiconductor melts with free capillary surfaces, particularly silicon crystal growth by the floating zone method. The effect of fluid motion due to the gravity and surface tension is illustrated. The axysymmetric Navier- Stokes and energy equations with Boussinesq approximation have been discretized by means of finite volume procedure, and the SIMPLER algorithm is used to treat the coupled velocity-pressure equations. A new flux type model for the temperature at the free surface models the heat experimental conditions. Different steady thermocapillary flows are obtained by varying the following significant parameters: temperature gradient conditions (Grashof number), surface tension gradient (Marangoni number), all of them relevant in practical crystal growth situations.

Keywords: Thermocapillary-driven flow, Buoyancy-driven flow, Crystal growth, Floating zone technique, Numerical simulation.

[1] Corresponding author. *Department of Applied Sciences, University of Quebec at Chicoutimi, 555, boul. de l'Université, Chicoutimi, Quebec G7H 2B1 Canada*, Tel.: +418-545-5011 ext.2470; Fax: +14185455012, E-mail: ryounsi@uqac.ca

1. INTRODUCTION

The design and optimization of modern materials processing systems rely on the understanding of some basic mechanisms and their interactions. Until years 50, the main method used in crystal growth was Czochralski (CZ) method, making call for growing solid crystals from a melt, (Kobayashi (1998), Mihelcic et al. (1981), Crochet et al. (1983) and Derby et al. (1989)). However, the advent of semiconductors drove researchers to invent proceed which is adapted to the industrial needs. The float-zone technique is one of the candidate methods for growing single crystals. The main advantage of the float-zone process is that it is a container-less process and thus a main source of contamination is removed. Another advantage is the reduction of thermal stresses which are caused by differential thermal expansion between the crystal and the crucible. Considerable attention has been paid in recent years to surface tension-driven convection in liquid floating zones and similar configurations under microgravity conditions. Kobayashi (1998) computed thermocapillary convection under zero gravity conditions for two different Prandtl numbers, with and without crystal rotation while neglecting the deformation of the free surface. Kobayashi (1998) extended the study to include buoyancy-induced convection. Young and Chait (1990) has presented asymptotic solutions for the temperature, concentration and interface shapes in the limit of small aspect ratio and weak surface tension for a two-dimensional float-zone established in a vertical sheet. Neitzel *et al*. (1990) have computed thermocapillary convection in a float-zone with a computed free surface shape. Chu and Chen (1995) have obtained numerical solutions for float-zone growth of Molybdenum (Mo) crystals with an imposed heat input profile rather than an imposed temperature profile. Monti (1987) investigated the onset of instability of Marangoni convection in space by using large liquid bridges with lengths of the order of several centimetres and in the absence of buoyancy effects. Recent experimental works have been performed by Petrov *et al*. (1996), Muehlner *et al*. (1997) and Schwabe *et al*. (1996).

In this method, a melted zone is obtained by melting, is maintained by its own superficial tension between two verticals solid and collinear. The superior cylinder is a polycrystalline solid, whereas the bottom one is a monocrystal, that growth as the melted zone recrystallise under the action of the vertical displacement of the lateral heating source. Two of the most important mechanisms are momentum transfer and heat transfer, which control such phenomena as fluid flow and solidification. The development of computational resources and numerical methods make computer modeling one of the major ways of studying this mechanism. In the industrial configuration of crystal preparation effected in soil, the melted phase is the seat of convective movement due to gravity and surface tension. The study of these coupled phenomena is revealed of big complexity. For this reason, we have examined every type of convection separately in order to understand the own dynamics of each.

The aim of this article is to characterize the flows of convection that could be observed. The numerical analysis of the flow in the melt is quite complex and simplified models are commonly used, where both the geometry and the thermal boundary conditions are simplified. A mathematical model for the flow and heat transfer during the floating-zone growth process is developed. The temperature and flow fields in the melt are obtained numerically. Natural and thermocapillary convection effects in the melt are included in the analysis.

2. MATHEMATICAL MODEL

In this work, the case of steady, axysymmetric flows in semiconductor melts is considered. The geometrical configuration considered is schematically shown in figure1. The floating zone is

modeled as a cylindrical liquid bridge (silicon melt) of radius R and length H, hold between two circular disks. The simulation is based on the Boussinesq approximation. Thus, we study the motion of a laminar incompressible fluid in the presence of thermal buoyancy forces. The heat generated by viscous dissipation in the melt is neglected, the transport coefficients (viscosity ...) are assumed to be temperature independent.

With these assumptions, the generalised equation which predicts heat transfer as well as melt flows during a growth process, is adapted in a non-dimensional formulation for FZ crystal growth as follows (symbol explanation is referred to nomenclature):

$$\frac{\partial \Phi}{\partial t}+\frac{\partial}{\partial z}(u\Phi)+\frac{1}{r}\frac{\partial}{\partial r}(rv\Phi)=\frac{\partial}{\partial z}\left(\Gamma_\Phi \frac{\partial \Phi}{\partial z}\right)+\frac{1}{r}\frac{\partial}{\partial r}\left(r\Gamma_\Phi \frac{\partial \Phi}{\partial r}\right)+S_\Phi \qquad (1)$$

Where Γ_Φ and S_Φ are shown in table 1.

Φ	Γ_Φ	S_Φ
1	0	0
u	1	$-\frac{\partial P}{\partial z}+\frac{\partial}{\partial z}\left(\frac{\partial v}{\partial z}\right)+\frac{1}{r}\frac{\partial}{\partial r}\left(r\frac{\partial u}{\partial z}\right)+Gr\Theta$
v	1	$-\frac{\partial P}{\partial r}+\frac{\partial}{\partial z}\left(\frac{\partial V}{\partial r}\right)+\frac{1}{r}\frac{\partial}{\partial r}\left(r\frac{\partial u}{\partial r}\right)$
Θ	$1/Pr$	0

Table1: Governing differential equations.

Where (u, v) is the fluid velocity, P is the pressure and Θ is the temperature. Gr is the Grashof, which characterise the intensity of convection, Pr is the Prandtl number.

In order to complete the mathematical model, we still use, in addition to equation 1, the appropriate boundary conditions. They are as follows:

at the bottom surface : $z=0;\ 0\le r<1$

$$u = v = \Theta = 0 \qquad (2)$$

at the top surface : $z=A;\ 0\le r<1$

$$u = v = \Theta = 0 \qquad (3)$$

at the free surface (right): $r=1\ ;\quad 0\le z\le A$

$$v=0\ ,\quad \frac{\partial u}{\partial r}=-\frac{Ma}{Pr}\frac{\partial \Theta}{\partial z}.(1-(z-1)^2)^2,\quad \frac{\partial \Theta}{\partial r}=(1-(z-1)^2)^2=0 \qquad (4)$$

at the symmetry axis (left): $r = 0$; $0 \le z \le A$

$$v = 0\,, \quad \frac{\partial u}{\partial r} = 0\,, \quad \frac{\partial \Theta}{\partial r} = 0 \tag{5}$$

The dimensionless stream function is evaluated in order to ascertain the strength of the convective motion and is defined in the usual way:

$$v = -\frac{1}{r}\frac{\partial \psi}{\partial z} \quad \text{and} \quad u = \frac{1}{r}\frac{\partial \psi}{\partial r} \tag{6}$$

A control volume based discretisation method, described by Patankar (1980) has been applied for solving the system of equation (1), together with the boundary and interfacial conditions (2-5). The most attractive feature of the control volume based discretisation scheme is that the resulting solution would imply that integral conservation of physical quantities such as mass, momentum and energy is exactly satisfied, over any group of control volumes and, of course, over the whole calculation domain. In evaluating convective and diffusive fluxes, a power-law scheme and the SIMPLER algorithm were considered. The choice of the convergence criterion is particularly important. Use of 51x5l non-uniform grid (figure 1) permits the presence of several discretisation points near the interface without introducing an excessive number of grid points, which would induce high CPU cost. The iterations were terminated when the residual sources of mass become less than 10^{-5}.

3. RESULTS AND DISCUSSION

In this section we study the character of the melt flow and the temperature field. Streamlines, velocity vector and isotherms are presented in the steady state case. In all of this study, the Prandtl number has a constant value Pr=0.0l5 corresponding to liquid metals (silicon) and aspect ratio A=2. The ranges of the other parameters studied herein are: $10^3 \le Gr \le 10^6$; $10 \le Ma \le 10^3$

3.1 Effect of buoyant convection

We first consider the influence of natural convection on the flow when thermocapillary forces are absent by setting Ma = 0. Natural convection is induced by an adverse or destabilising temperature gradient. The effect of the gravity is represented through the Grashof number. We have reported in figure 2 the flow pattern for several values of Grashof number (Gr). For very low values of Gr (not presented here), no flow is detected in the melt ($\Psi_{max} \sim 0$); the heat transfer is still dominated by conduction. As shown, one large vortex, which rotates counterclockwise in direction, dominates the flow field. It is caused by the ascending flow near the free surface the melt is directly heated by the outer heat source. Since the buoyancy grows larger as the increase of gravitational acceleration (Grashof number), the intensity of natural convection becomes highest at $Gr=10^6$ ($\Psi_{max}=240$). This is confirmed by the number of isolines in the stream function, which increases with the magnitude of Grashof number. On the contrary, the maximum temperature becomes lowest at $Gr=10^6$ due to a strong stir. The thermal convection destroys the symmetry with respect to the horizontal midplane. This observation is confirmed in figure 3 and figure 4, in which we have reported the axial velocity and temperature profiles at the free surface versus Grashof number. The maximum of temperature is slightly displaced to the top of the crystal.

3.2 Effect of thermocapillary convection

In this calculation, we consider only the effects of tension forces; a non-buoyant forces is imposed by setting Gr=0. This convection is obtained in experiences achieved in microgravity environment. Figure 5 illustrates typical streamlines, isotherms and velocity vector patterns for Gr=0 and Ma=10,10^2 and 10^3, respectively. Two vortices occupy the flow field as shown in figure 5(a), and are symmetrical with respect to the central height of the melt zone due to no buoyancy force. The vortices on the top and the bottom, which rotate counterclockwise and clockwise, respectively, are formed by the Marangoni effect on the free surface. For the temperature field it doesn't present a difference with conductive field. As the Marangoni number increases, the flow filed intensifies and the convective strength that comes with the increases of the Marangoni number modifies slightly the temperature filed. Since the fluid with high temperature on the free surface is moved to the low-temperature regions by the gradient of surface tension, the temperature gradient becomes steeper in the vicinity of the Marangoni convection. As a result, the rims of the free surface are gradually moved to the solid phases (horizontal walls, top and bottom) which maintained at a constant temperature. The coupling temperature-velocity at r=1 (free surface) explains the evolution of the axial velocity that is more and more reduced near of these cold walls as depicted in figures 6 and 7.

CONCLUSION

Flow and heat transfer in the melt, during floating zone growth of silicon, have been studied numerically. The model considered here, with a condition of flux and no temperature represents a new approach for the applied conditions of heating. We have analysed the structures of the flow of pure Marangoni convection and gravitational convection. The main conclusions of this study are summarized as follows:

- The structures of the flow are very dependent of the Marangoni number and where the temperature progresses slightly.
- In case of buoyant convection, the evolution of the flow with Grashof number is monotonous.
- The present analysis is focused on the influence of a limited number of dimensionless parameters. As an extension of this work, it is particularly relevant to take into account the effect Prandtl number (liquid melt) and combined buoyant and thermocapillary convections.

REFERENCES

Crochet, MJ., Wouters, PJ., Geyling, FT. and Jordan, AS., (1983) Finite element simulation of Czochralski flow. J. Cryst. Growth, 65, pp. 153-165

Chu CF. and Chen JC., (1995) Numerical computation of fluid flow of floating-zone crystal growth of molybdenum. Int. J. Heat Mass transfer, 38, pp. 1841-1853

Derby, JJ., Atherton, LJ., Thomas, PD. and Brown, RA., (1998) Finite element method for analysis of dynamics and control of Czochralski crystal growth. J. Scientific Computing , Vol. 2, pp. 297-343

Kobayashi, N., (1978) Computational simulation of the melt flow during Czochralski growth. J. Cryst. Growth, Vol. 43, pp. 357

Kobayashi, N., (1988) Steady convection caused by the temperature inhomogeneity in a cylindrical floating zone. Japan J. Appl. Phys., Vol. 27, pp. 20-24

Monti, R., (1987) On the Onset of the Oscillatory regimes in marangoni flows. Acta Astronautica; Vol. 15, pp. 557–560

Muehlner, KA., Schatz, MF., Petrov, V., McCormick, WD., Swift, JB., Swinney, HL., (1997) Observation of helical traveling Wave convection in a liquid bridge. Physics and Fluids; Vol. 9, n 6, pp. 1850–1852

Mihelcic, M., Schroeck-Pauli, C., Wingerath, K., Wenzl, H., Uelhoff, W. and Vander Hart, A., A (1981) Numerical simulation of forced convection in the classical Czochralski method, in ACRT and CARCT. J. Cryst. Growth, Vol. 53, pp. 337-354

Neitzel, GP., Hyer, JR. and Jankowski, DF., (1990) Thermocapillary convection in a model float-zone". AIAA Paper No. 90-0406

Petrov, V., Schatz, MF., Muehlner, KA., Van Hook, SJ., McCormick, WD., Swift, JB., (1996) Experimental control of thermocapillary convection in a liquid bridge. In Third Microgravity Fluid Physics Conference, NASA CP 3338, pp. 487–492

Patankar, SV., (1980) Numerical Heat Transfer and Fluid Flow, Hemisphere, Washington DC, USA

Schwabe, D., Hintz, P., Frank, S., (1996) New features of thermocapillary convection in floating zones revealed by tracer particle accumulation structures. Microgravity Science and Technology, Vol. 9, pp. 163–168

Young, GW., and Chait, A., (1990) Surface tension driven heat, mass and momentum transport in a two-dimensional float zone. J. Crystal Growth, Vol. 106, pp. 445-466

Nomenclature

A: aspect ration of the floating zone
g: gravity acceleration
Gr: Grashof number (buoyancy forces on viscous diffusion ratio)
Ma: Marangoni number (thermocapillary forces on thermal diffusion)
P: dimensionless pressure
Pr: Prandtl number (viscous on thermal diffusions ratio)
r, z: radial and vertical coordinates
R, H : radius and height of the floating zone
u, v: dimensionless axial and radial velocities

Subscripts

m: melt

Greek symbols

β: expansion coefficient of the melt
ν: kinematics viscosity
Θ: dimensionless temperature
Ψ: stream function
γ: surface tension for interface

List of Figures

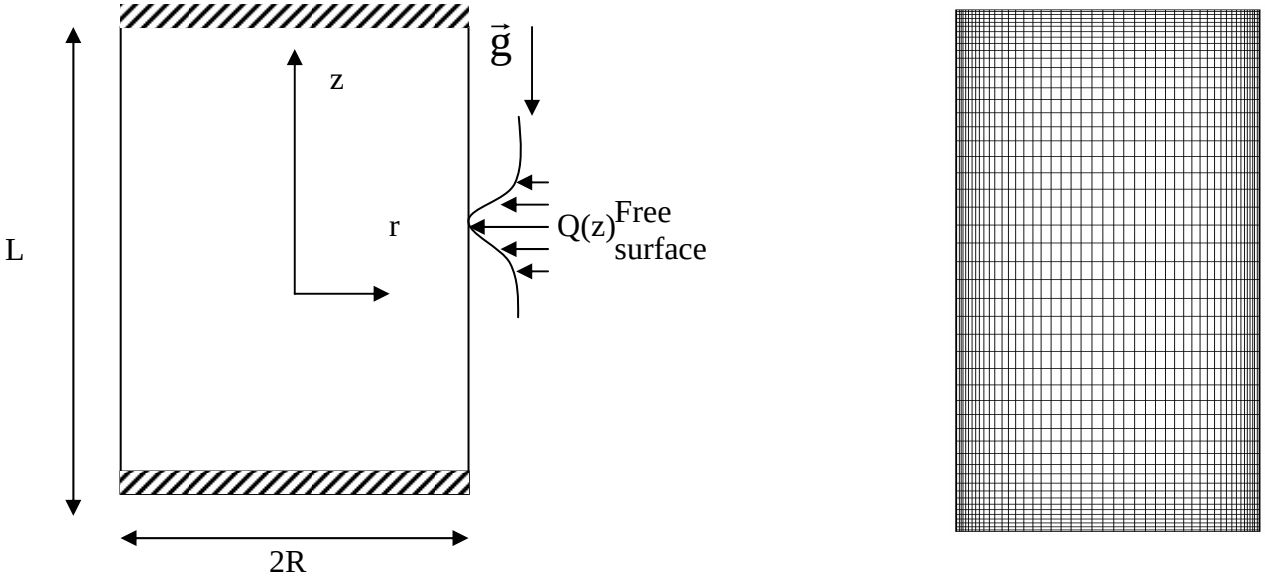

Figure 1: Schematic diagram of the floating zone system and mesh.

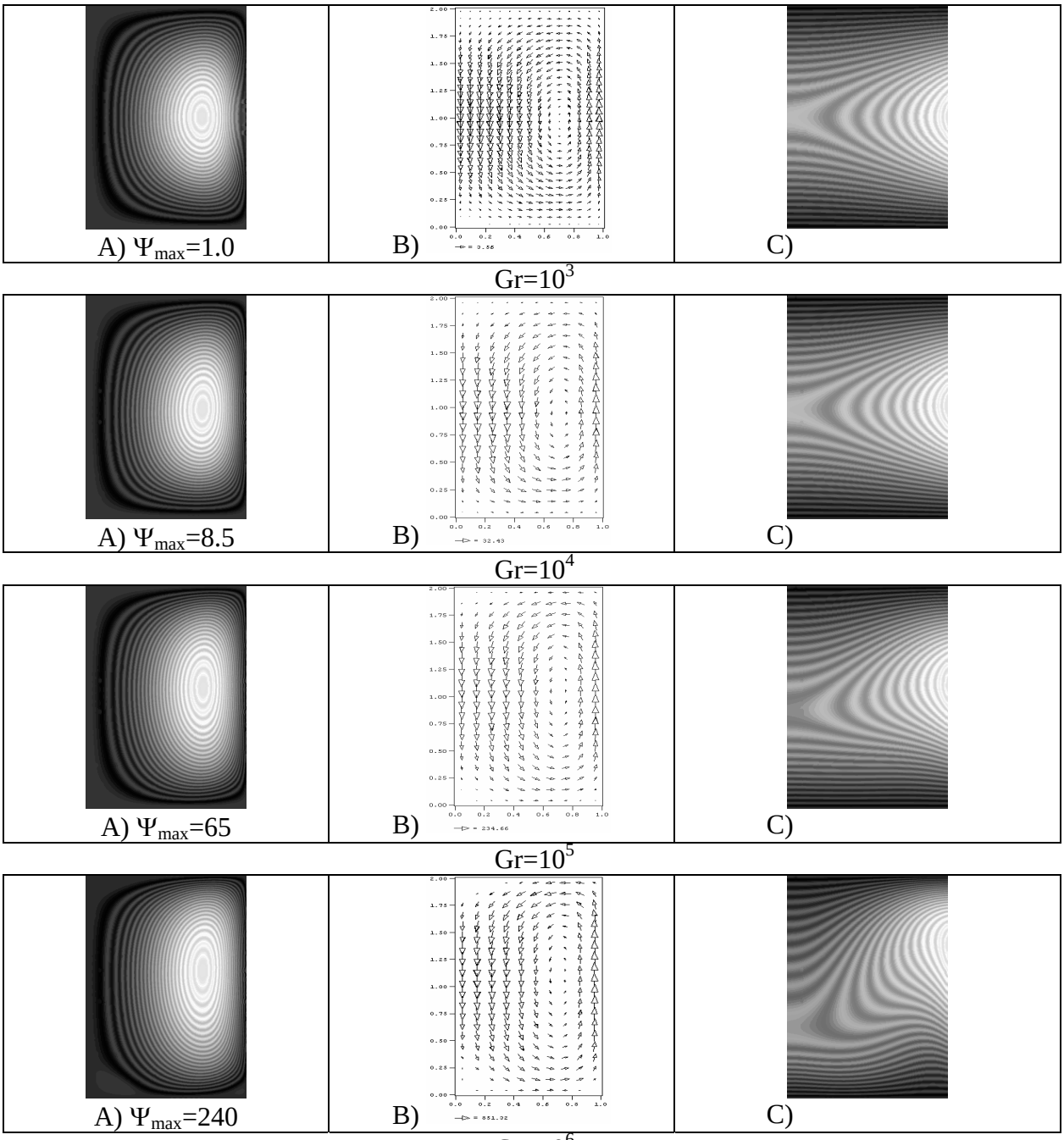

Figure 2: Effect of buoyant convection on: A) Streamlines, B) velocity vector, C) Isotherms. Pr=0.015, A=2, Ma=0

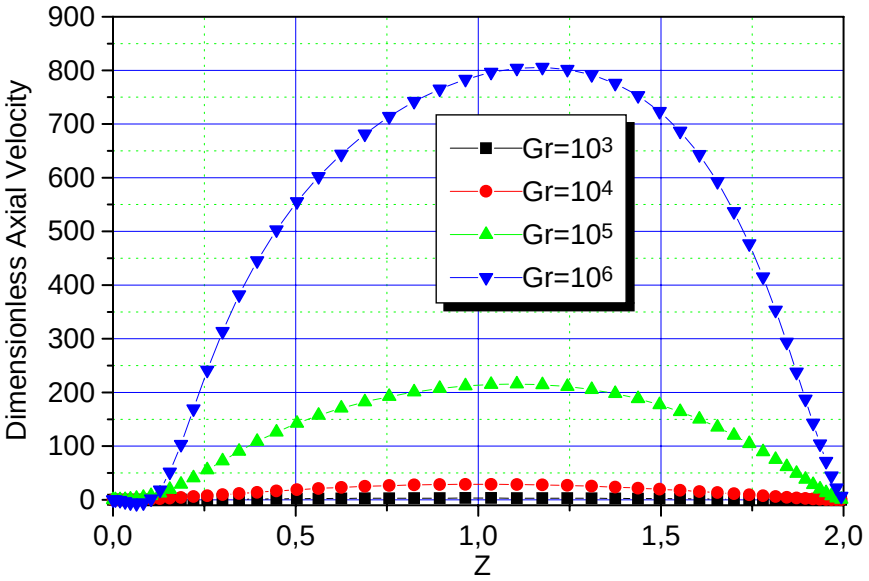

Figure 3: Profile of dimensionless axial velocity at the free surface versus Grashof number, Pr=0.015, A=2, Ma=0.

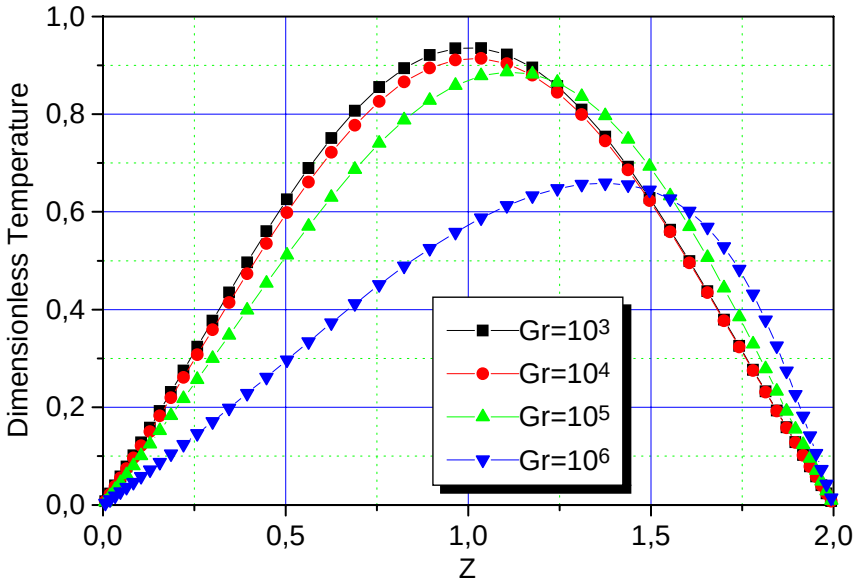

Figure 4: Profile of dimensionless temperature at the free surface versus Grashof number, Pr=0.015, A=2, Ma=0.

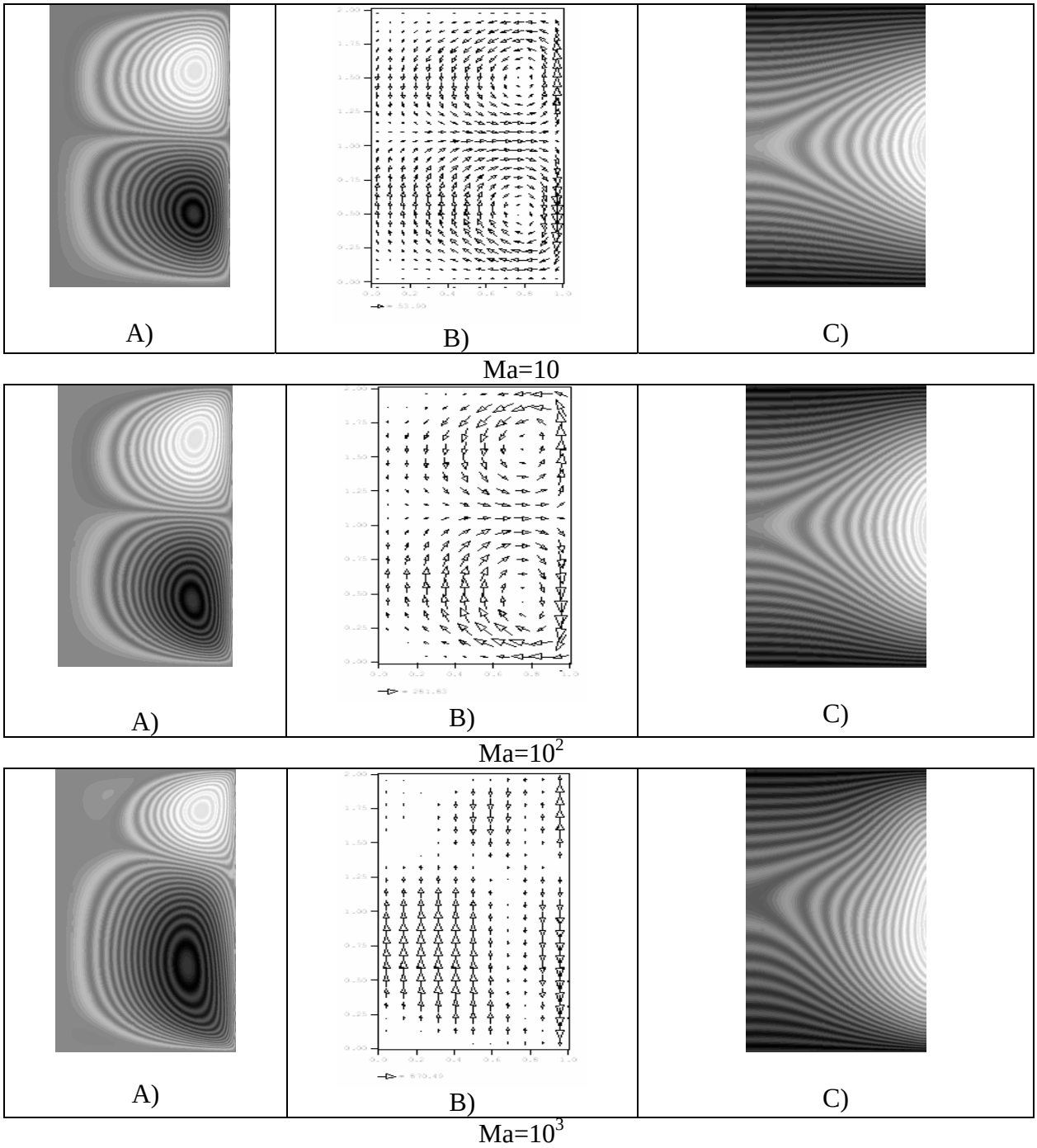

Figure 5: Effect of thermocapillary convection on: A) Streamlines, B) Velocity vector, C) Isotherms. Pr=0.015, A=2, Gr=0.

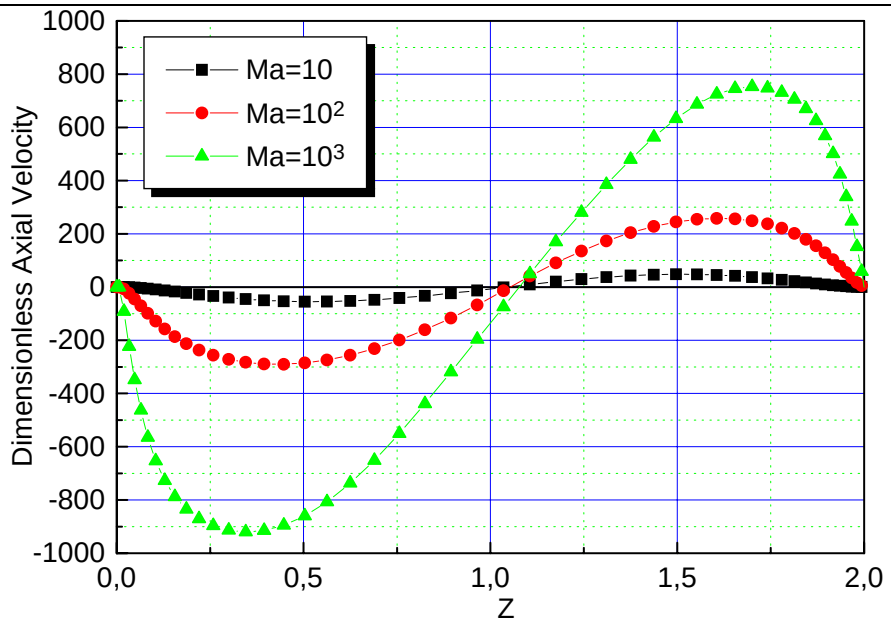

Figure 6: Profile of dimensionless axial velocity at the free surface versus Marangoni number, Pr=0.015, A=2, Gr=0.

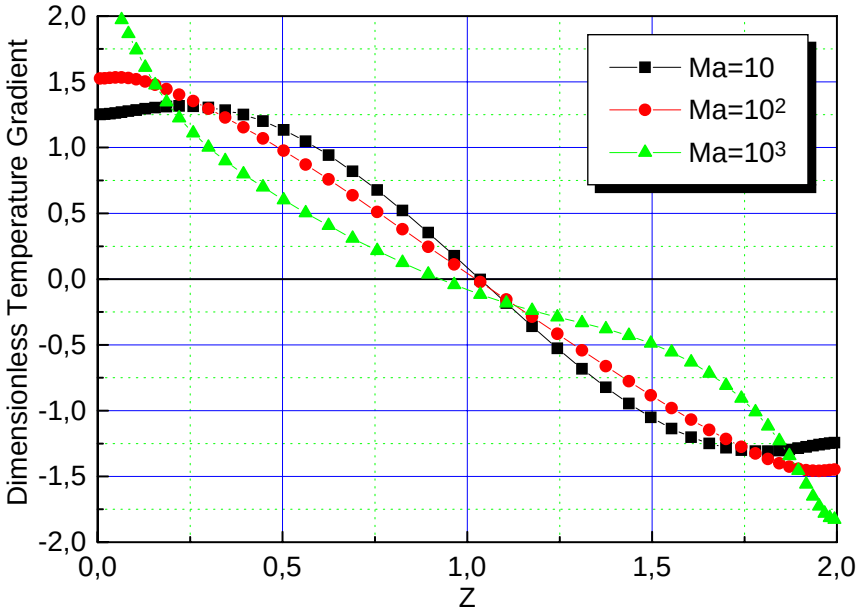

Figure 7: Profile of dimensionless temperature gradient at the free surface versus Marangoni number, Pr=0.015, A=2, Gr=0.